Scientific Journal for the Faculty of Science-Sirte University

Journal home page: http://journal.su.edu.ly/index.php/JSFSU/index

DOI: 10.37375/issn.XXX-XXX

Theoretical Study of Electron Phonon Interactions Using Linear Response Theory

Nadir Omar Massoud Driza, Asma R.S. Elgade, Rafa S. A. Hamad, and Hanan M. A. Ali

Department of Physics Universtiy of Benghazi faculty of Arts and Sciences Elmarj

DOI:https://doi.org/10.37375/sjfssu.v5i2.3351

ARTICLE INFO:

Received: 01 June 2025

Accepted: 0 1 August 2025

Published: 27 October 2025:

Keywords:
Electron, Phonon interactions, linear Response theory, transition metal

A B S T R A C T

This work presents a theoretical investigation of electron–phonon interactions in transition metals using linear response theory, with the aim of evaluating the agreement between ab initio calculations and experimental data. The study focuses on aluminium (Al), molybdenum (Mo), and niobium (Nb), utilizing a wave-vector-dependent approach to calculate the electron–phonon coupling. The linear muffin-tin orbital (LMTO) method combined with the local density approximation (LDA) was employed to evaluate the screening of the one-electron potential within the framework of linear response theory. From these calculations, key physical parameters, including electron–phonon coupling strengths and transport coefficients, were extracted. The theoretical results show a strong correspondence with experimental measurements, demonstrating the reliability of the linear response approach in capturing electron–phonon coupling behaviour in these metals. These findings support the broader applicability of first-principles methods in the study of phonon-mediated transport phenomena in metallic systems.

1 Introduction

Many features of metals, including their electrical and thermal resistivities, superconductivity, and the renormalization of the linear electronic specific heat, are determined by the electron-phonon interaction [20] [10]. Within the framework of the strong coupling theory of superconductivity, the electron-phonon spectral distribution function α2 F(ω) and its initial reciprocal moment λ are essential quantities. It is particularly challenging to compute λ ab initio for the quantitative understanding of high-temperature superconductivity. In order to determine the whole low-energy excitation spectrum of 2.the metal, including the quasiparticle energies Ekj and the phonon frequencies ωqv, it is necessary to establish a method for calculating this value that is widely applicable. The one-electron band structure derived from a local-density approximation (LDA), utilizing density functional computation is the most commonly used estimate of Ekj. 1. Therefore, we make clear that we used linear response theory and first-principles technique to calculate electron-phonon interactions inside the linear muffin-tin orbital (LMTO) framework. Their approach, based on density functional perturbation theory (DFPT) and the local density approximation (LDA), enabled the evaluation of wave-vector-dependent electron–phonon coupling in metallic systems. This work represented a significant advancement in the field by providing accurate, parameter-free predictions of phonon spectra, coupling strengths, and transport coefficients for materials such as Al, Mo, and Nb. The close agreement between theoretical results and experimental measurements demonstrated the reliability of the method and established a foundation for subsequent developments in ab initio studies of phonon-mediated phenomena, including superconductivity and electronic transport.2.

Corresponding author: E-mail: nadir.driza@uob.edu.ly

Theory

In this article we utilize a linear muffin-tin orbital (LMTO)–based implementation of Density Functional Perturbation Theory (DFPT). Specifically, our work uses a full-potential LMTO code (often referred to as LMTART, developed by Savrasov in Max Planck institute, Stuttgart university which is specific simulation program), which supports linear-response calculations for phonons and electron–phonon coupling. This approach allows us to compute phonon dispersion and electron–phonon matrix elements directly through the Sternheimer equation and evaluate the screening of the one-electron potential under small lattice perturbations, using the local-density approximation (LDA) within LMTO.

In this work, we used the linear-response theory (Winter, 1981) (Savrasov, 1996) for the screening that has been applied to calculate λ on the case of aluminium and it was a great fit (Winter, 1981). Primarily, the calculation of λ was focused on calculating the "electronic contribution" in many previous attempts, especially for transition metals (Chung, 2017). The phonon frequencies and eigenvectors were typically derived from inelastic neutron-scattering data. However, understanding how electrons react to atomic vibrations (phonon distortion) in ideally requires a complex, "self-consistent" calculation of their energy potential. Therefore, such computational demands led us to employ approximations like the rigid-ion (RIA) or rigid-muffin-tin (RMTA) methods (Salunke, 1997; Gaspari, 1972; Van Loon, 2018). While these simplified models made calculations feasible, later linear-response theory revealed a crucial insight: these approximations are often not universally accurate, prompting the development of more precise approaches.

None the less, the frozen-phonon total-energy approach utilizing supercells can calculate accurate phonon frequencies and eigenvectors, as well as the self-consistent screening and, consequently, the electron-phonon interaction, but only for commensurate phonon wave vectors q, (Dacorogna, 1985) (Cohen, 1990) (Liechtenstein, 1991). Since the supercell's restricted size permits crude sampling, the accuracy of q-integrated quantities such as λ is typically insufficient to estimate, for example, T_C.

On the solid-state, the Sternheimer method (Shang, 2021) (Welakuh, 2022) is one of an effective linear-response approaches for transition metals that was utilized to generate precise phonon dispersions and eigenvectors for any arbitrary q (Savrasov, 1992). A significant advantage of this method lies in its use of muffin-tin basis sets for electron wave functions, rather than traditional plane-wave basis sets. This strategic choice enables the method to effectively treat systems encompassing narrow bands, such as d bands, with the same ease and accuracy as those characterized solely by broad bands. We extend this approach to the computation of the wave-vector dependent electron-phonon interaction in the current paper. When neither the Rigid Muffin-Tin Approximation (RMTA) nor the Random-Phase Approximation (RIA) is employed, a crucial aspect of our calculations involves the self-consistent determination of the screening potential. This iterative process ensures that the potential accurately reflects the system's response to an external perturbation for every momentum component q. Integration across the complete Brillouin zone yields $\alpha^2 F(\omega)$ and λ. We show that this all-electron method is applicable by calculating $\alpha^2 F(\omega)$ for a few elemental metals, namely the d-band metals Nb and Mo, and the sp-band metal Al. Additionally, we report the results for the thermal and electrical resistivities at 273 K that are phonon-limited, as well as the dimensionless λ_{tr}. These are the first fully screened ab initio calculations for the d-band metals as we see in the next equation:

$$\alpha^2 F(\omega) = \frac{1}{2\pi N(0)} \sum_{q\nu} \frac{\gamma_{q\nu}}{\omega_{q\nu}} \delta(\omega - \omega_{q\nu}) \qquad (1)$$

with respect to the phonon linewidths $\gamma_{q\nu}$,, resulting from the electron-phonon interaction, for $\alpha^2 F(\omega)$. We refer to atomic Rydberg units here and in the following. Σ_q is the average over the Brillouin zone (BZ), ν stands for the phonon branching, and $N(0)$ is the electronic density of states per atom and per spin at the Fermi level. In cases when the energy bands surrounding the Fermi level exhibit linear behaviour throughout the phonon energy range, the Fermi "golden rule" provides the linewidths and it could be expressed as in the next equation:

$$\gamma_{q\nu} = 2\pi\omega_{q\nu} \sum_{kjj'} \delta(E_{kj}) \delta(E_{k+qj'}) \left| g^{q\nu}_{k+qj',kj} \right|^2 \qquad (2)$$

The band indices are denoted by j and j', the electron-phonon matrix element is $g^{q\nu}_{k+qj',kj}$, and the energies with respect to the Fermi level are represented by E_{kj}. The probability of scattering via the phonon $q\nu$ from the one-electron state $|kj\rangle$ to the state $|k+qj\rangle$ is the traditional definition of g. This expression presents an evaluation challenge when electronic states are approximated by

superpositions of atom-centered orbitals. This is primarily due to its dependence on orbitals defined at the equilibrium atomic positions while simultaneously incorporating the potential of the displaced lattice. The rationale is that, by applying the Rayleigh-Ritz variational principle with a finite orbital basis $|x_\alpha^k\rangle$, the states $|kj\rangle$ in the band calculation are derived as the best approximation for the equilibrium locations rather than as accurate solutions of the one-electron Schrödinger equation. The dynamical matrix calculation now includes significant incomplete-basis-set (IBS) corrections (Savrasov, 1992). The electron-phonon matrix elements need to be evaluated while accounting for the IBS factors. By simply repeating the conventional quantum-mechanical method of deriving the Fermi golden rule, they can be found: The overlap integral squared represents the scattering rate for changes from an initial, unperturbed state to a final, perturbed state. When considering a displaced lattice, the final state's optimal variational estimate requires orbitals that are both centered at the new atomic positions and adapted to the new one-electron potential. This results in the change in the basis $|x_\alpha^k\rangle$ being found to linear order with regard to the displacements. For the purposes of equation (2), the definition of g is therefore

$$g_{k+qj',kj}^{q\nu} = \langle k+qj'|\delta^{q\nu}V|kj\rangle + \left\langle \sum_\alpha \delta^{q\nu}\, x_\alpha^{k-q} A_\alpha^{k+qj'} \middle| H - E_{kj} \middle| kj \right\rangle + \left\langle k+qj' \middle| H - E_{kj} \middle| \sum_\alpha \delta^{q\nu} x_\alpha^k A_\alpha^{kj} \right\rangle \quad (3)$$

where A_α^{kj} are the coefficients of I $|x_\alpha^k\rangle$ in the expansion of $|kj\rangle$, and $\delta^{q\nu}x_\alpha^k$ and $\delta^{q\nu}V$ are the basis and one-electron potential changes caused by the phonon distortion, respectively (Savrasov, 1992). The frozen-phonon supercell approach has been described (Liechtenstein, 1991), which splits the bands to evaluate $g_{k+qj',kj}^{q\nu}$. The linear-response analogy of this process was found in equation (3). It has a proper long wavelength behaviour, helps one to avoid including d—f transitions in at-electron systems, and is less susceptible to the inaccuracies in the wave functions introduced by the variational principle. The second and third contributions in (3) are associated with the IBS corrections. They vanish for plane-wave basis sets, but as we will see, they should be considered when employing linear augmented-plane-wave (LAPW) and muffin-tin-orbital (LMTO) bases (Andersen, 1975).

For phase-space considerations, such as Fermi-surface nesting, the phonon linewidths $\gamma_{q\nu}$ eq. (2) frequently exhibit rapid changes over the BZ (Butler, 1979). As a result, the summation of q in equation (1) for $\alpha^2F(\omega)$ must be carried out on a relatively dense mesh. However, since the phonon frequencies $\omega_{q\nu}$ are essentially smooth functions of q, they shouldn't be calculated on a mesh with this level of density. Our method is predicated on converting the dynamical matrix to real space: Initially, we computed the self-consistent linear response of $\omega_{q\nu}$ for 10 specific q points using the LDA-LMTO method (Savrasov, 1992).

A double-k spherical-harmonics basis set with a large number of k points was used for each electronic-structure computation. The complete potential and the wave functions one-center spherical-harmonics expansions were carried up to l_{max}= 8 (Savrasov, 1992). Next, we built the dynamical matrix on the real-space lattice T by summing over the 10 q points with the factor $e^{iq.T}$.

The phonon frequencies and eigenvectors for any q were eventually obtained using inverse Fourier summation and subsequent diagonalization. To determine α^2 F(ω) and λ, the phonon linewidths for 47 q sites were calculated. Using a modest setup (47 k points instead of 256 and a single-z LMTO basis set), the self-consistent screening potential $\delta^{q\nu}V$ was discovered for each, introducing just a (1—2)% inaccuracy of the final results. Utilizing the fullzone tetrahedron approach (Allen, 1983), a very large number of k points (752) were used to achieve the k-space integration in (2) involving the two δ functions. The q-space integration in (1) caused the biggest numerical inaccuracy of $\alpha^2F(\omega)$.

3. RESULTS AND DISCUSSION

The results we obtained ab initio for Al are presently being discussed. When compared to the tunneling measurements (Wolf, 2012), Fig. 1 displays the computed $\alpha^2F(\omega)$ (full line) compare with the tunneling measurements (small squares). It is comparable to the two curves. The empirical pseudopotential finding (Papaconstantopoulos, 1977) based on the rigid-ion approximation is found to be extremely close to our $\alpha^2F(\omega)$ value. Our results for the dispersion of $\gamma_{q\nu}$ along the high-symmetry directions likewise show general agreement with the ab initio frozen-phonon results (Dacorogna, 1985). With one possible exception, our longitudinal branch is twice longer than theirs in the [110] direction. This difference is likely related to the Gaussians that employed to replace the δ functions in (2). However, it turns out that our high γ values have a

very tiny relative weight in the integrated quantity. As we know, Understanding the electron-phonon coupling constant (λ) is crucial for characterizing the properties of various materials, particularly in superconductivity and charge transport. This basic parameter has been compellingly illuminated by recent experimental and theoretical studies.

Tunneling experiments, as reported by Wolf (2012), have yielded a λ value of 0.42. This experimental determination provides a valuable benchmark for comparison with theoretical predictions. Intriguingly, our own calculations have resulted in a λ value of 0.44 (see Table I for a detailed comparison). The striking similarity between these two values—one derived from direct experimental observation and the other from our computational approach—lends significant credibility to both methodologies. Further reinforcing these findings, earlier theoretical efforts also align closely. Linear-response calculations, performed by Winter (1981), estimated λ to be 0.38. Similarly, frozen-phonon calculations, as conducted by Dacorogna (1985), provided a value of 0.45. The convergence of these diverse approaches, encompassing both experimental and theoretical methodologies, underscores the robustness of the derived λ values for the material under investigation.

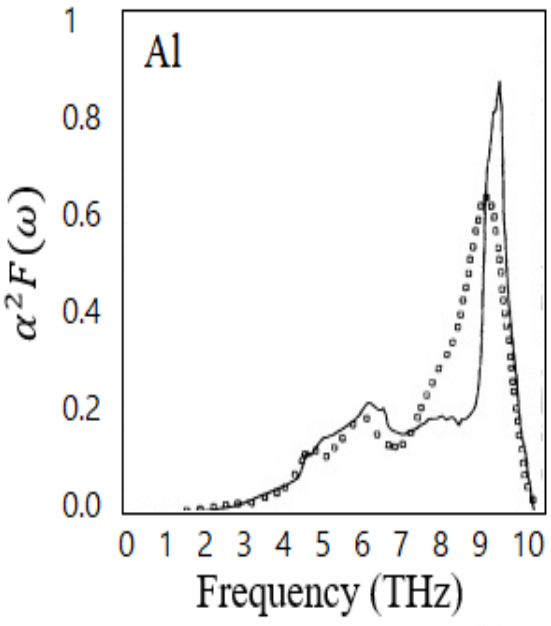

Figure (1) The spectral function $\alpha^2F(\omega)$ for Al, represented as a solid line, was calculated and compared with the tunneling data in squares (Wolf, 2012).

Our investigations into the electron-phonon coupling constant (λ) for Al yielded a value of 0.42. This deduction was made by utilizing our predicted density of states at the Fermi level, N(0)=2.74 states/(Ry spin), in conjunction with experimental specific-heat measurements.

Additionally, an independent calculation yielded λ=0.14. This calculation served to corroborate prior findings by Winter (1981) and Papaconstantopoulos (1977) concerning the applicability of the Rigid Muffin-Tin Approximation (RMTA) to sp metals. These results collectively contribute to a deeper understanding of electron-phonon interactions within this class of materials. The electronic transport parameter λ_{tr}, along with the electrical (ρ) and thermal (ω) resistivities at 273 K, are the additional computed values indicated in Table 1.

Based on the low-order variational estimate of the solution to Boltzman's equation, the computational approach is similar to that employed in superconductivity theory (Allen, 1978). Our computed transport spectral function, λ_{tr} =0.36, is close to the superconducting λ and does not show any qualitative differences from the standard one. In the analysis of our findings, a notable congruence emerged between the empirically measured values and the theoretically estimated figures for both ω and p. This strong agreement validates the predictive power of our models and the accuracy of our experimental methodologies.

Table 1. A direct comparison of several crucial parameters at 273 K to understand the intricate relationship between theoretical predictions and experimental observations in material transport, these include the thermal resistivity (ω, expressed in K cm/W), electrical resistivity (ρ, in μΩ), and the electron-phonon coupling constant (λ). Furthermore, the table presents calculated transport parameters (λtr). For Niobium (Nb), a breakdown of the electron-phonon coupling constant (λ) into contributions from its individual Fermi-surface sheets (octahedron, jungle gym, and ellipsoids) is provided in parentheses, drawing upon the foundational work by Crabtree (1979) and Wolf (2012). This detailed analysis highlights the contributions of specific electronic structures to the overall material behavior.

	Al	Nb	Mo
λ^{calc}	0.44	1.26 (1.44, 1.37, 1.08)	0.42
λ^{exp}	0.42	1.33 (1.71, 1.43, 1.10)	0.44
λ_{tr}^{calc}	0.36	1.17	0.35
ρ^{calc}	2.35	13.67	4.31
ρ^{exp}	2.43	13.30	4.88
ω^{calc}	0.42	2.17	0.73
ω^{exp}	0.42	1.93	0.72

Further, the latter proximity electron tunnelling spectroscopy (PETS) results are strongly confirmed by the curves in Fig. 2 (Geerk, 1982). Actually, these are made from sputtered Nb films that have been shielded from oxygen by an incredibly thin layer of Al deposition that happens right after the Nb deposition. The upper and lower spectra depicted in Fig. 2, corresponding to λ values of 0.97 and 0.96, correspond to substrate temperatures of 800◦C and < 75◦C, respectively.

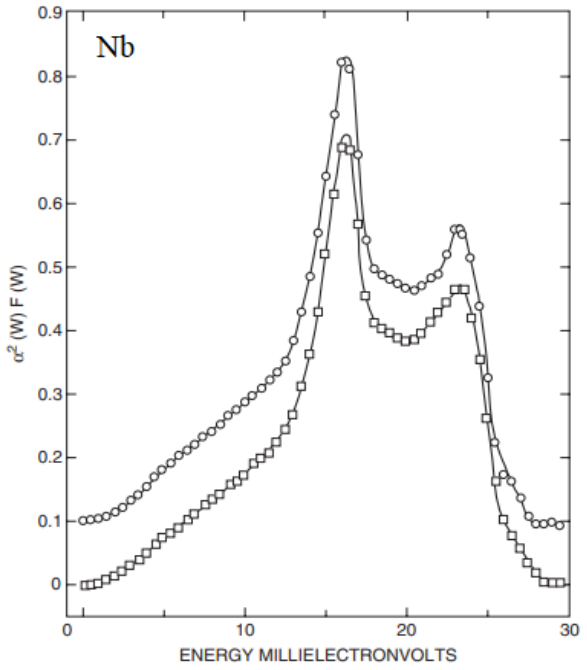

Figure 2 Sputtered Nb film tunneling $\alpha^2F(\omega)$: higher curve corresponds to a substrate temperature of 600 ◦C; lower curve represents ambient substrate temperature.

In Fig. 3, the solid curve replicates the $\alpha^2F(\omega)$ of (Khim, 1981), while the solid circles are *F(ω)* calculated from polycristalline Nb by (Gompf, 1981). This figure can be considered a definitive experimental comparison of *F(ω)* and $\alpha^2F(\omega)$, with the most notable feature being the apparent drop of $\alpha^2F(\omega)$ from about 3 meV at ω = 16 meV to about 1.9 meV at 24 meV. The tunnelling results from three different methods agree fairly well, and the neutron results shown here cannot be questioned on the grounds of the Born–von Karman interpolation [these are directly measured F(ω) points].

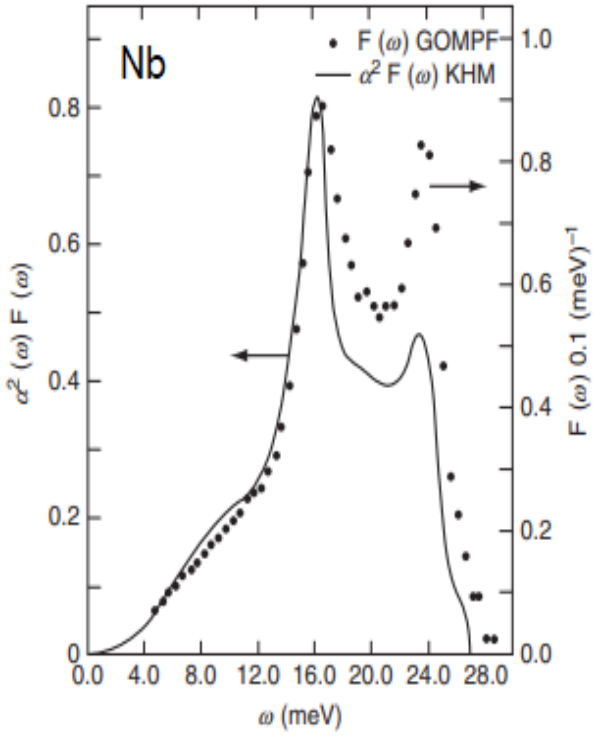

Figure 3 The incoherent inelastic neutron scattering on polycrystalline material was used to determine the Nb *F(ω)* (Since Gompf in 1981.)

This conclusion, as illustrated in Fig. 4, continues to deviate somewhat from theory. In this case, it would seem that α^2 (24 meV) ≈ 4.7 meV, more than twice the experimental value from the previous figure, is implied by the solid curve, which represents $\alpha^2F(\omega)$, calculated in a rigid muffin tin approximation (RMTA) method that incorporates experimentally determined phonon linewidths (Butler, 1979). In terms of absolute values, the estimated values of $\alpha^2(\omega)$ by (Butler, 1979) coincide with the experimental values at ω = 16 meV and below; these values are around 3 meV throughout the most of the spectrum, and may have a peak value of 4.5 meV in a limited region close to 22 meV.

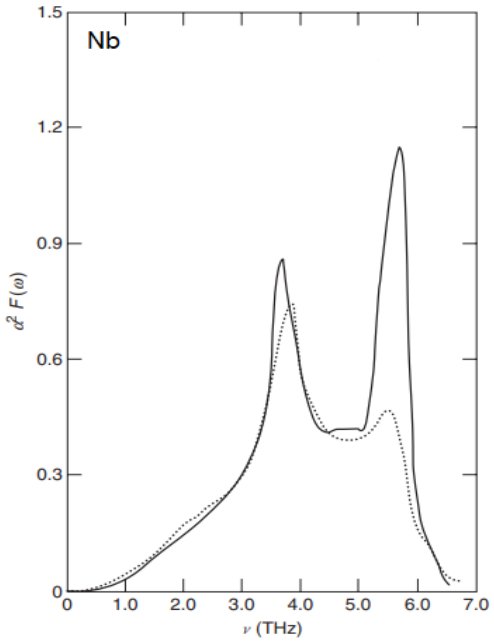

Figure 4 Determined Nb's $\alpha^2 F(\omega)$ using stiff muffin tin computations based on neutron scattering data. (Wolf, 2012) (Butler, 1979) Comparing the theoretical curve to the tunneling $\alpha^2 F(\omega)$, it is proven to be solid.

As we've seen, all of the tunnelling determinations now closely coincide, however there is a disagreement in the strength of the upper phonon peak in $\alpha^2 F(\omega)$ for Nb. The precise cause of the observed experimental anomaly remains unclear, but two primary possibilities are under consideration.

First, experimental limitations might play a role. As electron-phonon coupling increases around the 22 meV energy range, the effective sample depth appears to shrink relative to the electron's mean free path. This suggests that the finite size of the sample could be influencing electron behavior.

Second, the theoretical model's approximations could be a factor. The theory uses the stiff muffin tin approximation to calculate matrix components. This simplification of atomic potentials might not accurately capture the nuanced interactions of electron-phonon coupling, potentially leading to discrepancies between theoretical predictions and experimental observations. its exact cause is unknown, two possibilities include the experiment's decreasing sample depth with the mean free route as the electron-phonon coupling grows in the 22 meV area and the theory's use of the stiff muffin tin approximation to calculate the matrix components.

Among elemental superconductors, niobium (Nb) is one of the most researched. This significant research interest stems from a combination of comprehensive theoretical groundwork, a wealth of experimental data accumulated from prior investigations, and, critically, its comparatively high transition temperature (T_C) of 9.25 K. This relatively elevated T_C makes Niobium a particularly promising material for various superconducting applications, driving continued exploration into its fundamental properties and potential uses. Numerous theoretical calculations based on RMTA are available in the literature (Haque, 2017) (Mehl, 2001) and a wide range of λ (1.12—1.86) have been determined. Controversial have also been the tunnelling measures outcomes. The measured tunnelling data (Wolf, 2012) (small squares) and our computed $\alpha^2 F(\omega)$ (full lines) are compared in Fig. 4. The δ function in Eq. (1) should be a Lorentzian of half-width γ_{qv}, so the theoretical $\alpha^2 F(\omega)$ should be broadened. However, this tunneling experiment provides a coupling as gave by this value (λ_{tun}= 1.04) (Wolf, 2012), which is weaker than what we compute (λ=1.26). Using the RMTA, we get comparable results that are entirely consistent with previous estimates (Butler, 1979). As a result, we could confirm that the disparity would not be resolved by fully incorporating screening. An average mass augmentation of 1.33 is obtained by comparing our LDA band masses with those obtained from the de Haas — van Alphen (dHvA) effect (Crabtree, 1979). It is noteworthy, this value aligns strikingly with the 1.26 obtained through our electron-phonon calculation. This significant agreement not only validates our current findings but also reinforces the predictive power of the theoretical framework employed. A notable observation from our analysis is an enhancement factor of 1.3 when comparing the experimentally measured electronic specific heat coefficient with our calculated Local Density Approximation (LDA) density of states, N(0)=10.21 states/(Ry spin). This enhancement suggests the presence of significant many-body effects, such as electron-phonon coupling or electron-electron interactions, that contribute to the effective mass of the electrons beyond what is predicted by the bare band structure. A key contribution of this work is the detailed characterization of mass enhancement across a range of cyclotron orbits. While previous results from the Rigid Muffin-Tin Approximation (RMTA) have presented conflicting views, our measured variation of the mass enhancement for these distinct orbits demonstrates remarkable agreement with the predictions of our linear-

response calculation. This consistency, detailed in Table I, is a significant finding that validates our theoretical approach and highlights potential limitations or inaccuracies in the RMTA's applicability to this specific phenomenon. Dynamic screening and detailed band structure effects are crucial for accurately characterizing the observed mass gains in different orbital configurations, as demonstrated by the excellent correlation between our experimental data and linear-response models. The cyclotron masses and the electronic specific-heat coefficient are therefore enhanced by electron-electron interactions as well as electron-phonon interactions, which could mean that the tunneling data is still true and our estimate is incorrect. Nonetheless, Table I shows that our computed electrical and thermal resistivity values are reasonably close to the experimental values. Furthermore, there is a good agreement between the experimental value and the LDA value for the spin-lattice relaxation rate computed without any spin enhancement (beyond around 10%) (Asada. 1983). Therefore, it appears that the mass increase resulting from electron-electron interactions is less than 20% in Nb and that the electron phonon λ is 1.2—1.3. A Coulomb pseudopotential of $\mu^* \sim 0.2$ is needed instead of the lesser value ~0.14 that is often assumed (Savrasov, 1996) when using such a big λ value in conjunction with the measured T_C value in the McMillan formula (Xie, 2022).

Finally, we talk about Mo's outcomes. Due to its low T_C = 0.92 K and poor phonon effects, there are no tunneling data available for this material. It is discovered that our linear response calculations of $\alpha^2F(\omega)$ are in close agreement with previous results and our RMTA calculations (Wolf, 2012). Our total λ of 0.42 agrees well with the value of 0.44 that was obtained from McMillan's T_C expression using $\mu^* \sim 0.13$. The behavior of the computed transport spectrum function is extremely comparable to that of the superconductor ($\lambda_{tr} = 0.35$); Table I shows that our electrical and thermal resistivities are in close proximity to those that were measured.

4. CONCLUSION

In this study, we have performed self-consistent, ab initio linear response calculations of electron–phonon interactions for the elements Al, Nb, and Mo, using the local density approximation (LDA) within the linear muffin-tin orbital (LMTO) framework. The computed electron–phonon coupling strengths and transport parameters show good agreement with available experimental data - thermal resistivity ω, electrical resistivity ρ, and electron-phonon coupling constant λ at 273 K -, demonstrating the effectiveness and reliability of the approach for both broad- and narrow-band metals. These results underscore the viability of first-principles methods in accurately describing electron–phonon interactions across a range of metallic systems. However, discrepancies observed in the case of Nb, particularly when compared to tunneling data, suggest that additional theoretical and experimental investigations are warranted to fully resolve these differences and deepen our understanding of coupling mechanisms in superconducting materials.

Conflict of interest: The authors declare that there are no conflicts of interest

References

Allen, P. B. (1978). New method for solving Boltzmann's equation for electrons in metals. *Physical Review B, 17*(8), 3725–3734. https://doi.org/10.1103/PhysRevB.17.3725

Allen, P. B. (1983). A tetrahedron method for doubly constrained Brillouin zone integrals. *physica status solidi (b), 120*(2), 629–633. https://doi.org/10.1002/pssb.2221200209

Andersen, O. K. (1975). Linear methods in band theory. *Physical Review B, 12*(8), 3060–3083. https://doi.org/10.1103/PhysRevB.12.3060

Asada, T., & Terakura, K. (1983). Theoretical study of nuclear spin lattice relaxation in HCP transition metals. *Journal of Magnetism and Magnetic Materials, 31-34*, 45–46. https://doi.org/10.1016/0304-8853(83)90145-2

Butler, W. H., Pinski, F. J., & Allen, P. B. (1979). Phonon linewidths and electron-phonon interaction in Nb. *Physical Review B, 19*(8), 3708–3715. https://doi.org/10.1103/PhysRevB.19.3708

Chung, D. D. L. (2017). *Carbon composites: Composites with carbon fibers, nanofibers and nanotubes* (2nd ed.). Butterworth-Heinemann.

Cohen, R. E., Pickett, W. E., & Krakauer, H. (1990). Theoretical determination of strong electron-phonon coupling in $YBa_2Cu_3O_7$. *Physical Review Letters, 64*(22), 2575–2578. https://doi.org/10.1103/PhysRevLett.64.2575

Crabtree, G. W., Dye, D. H., Karim, D. P., & Koelling, D. D. (1979). Anisotropic many-body effects in the quasiparticle velocity of Nb. *Physical Review Letters, 42*(6), 390–393. https://doi.org/10.1103/PhysRevLett.42.390

Dacorogna, M. M., & Cohen, M. L. (1985). Self-consistent calculation of the q dependence of the electron-phonon coupling in aluminum. *Physical Review Letters, 55*(8), 837–840. https://doi.org/10.1103/PhysRevLett.55.837

Driza, N., Blanco-Canosa, S., Bakr, M., Soltan, S., Khalid, M., Mustafa, L., Kawashima, K., Christiani, G., Habermeier, H.-U., Khaliullin, G., Ulrich, C., Le Tacon, M., & Keimer, B. (2012). Long-range transfer of electron–phonon coupling in oxide superlattices. *Nature Materials, 11*(8), 675–681. https://doi.org/10.1038/nmat3378

Gaspari, G. D., & Gyorffy, B. L. (1972). Electron-phonon interactions, d resonances, and superconductivity in transition metals. *Physical Review Letters, 28*(13), 801–805. https://doi.org/10.1103/PhysRevLett.28.801

Geerk, J., Gurvitch, M., McWhan, D. B., & Rowell, J. M. (1982). Electron tunneling into Nb/Al multilayers and into Nb with Al overlayers. *Physica B+C, 109-110*, 1775–1784. https://doi.org/10.1016/0378-4363(82)90200-5

Gompf, F., Richter, W., Scheerer, B., & Weber, W. (1981). Phonons in superconducting Nb-Zr alloys: Experiment and theory. Physica B+C, 108(1-3), 1337–1338. https://doi.org/10.1016/0378-4363(81)90967-0

Haque, E., & Hossain, M. A. (2017). First-principles study of mechanical, thermodynamic, transport and superconducting properties of Sr_3SnO. *Journal of Alloys and Compounds, 730*, 279–283. https://doi.org/10.1016/j.jallcom.2017.09.299

Khim, Z. G., Burnell, D., & Wolf, E. L. (1981). Equivalence of optimized conventional and proximity electron tunnelling (PET) for niobium. *Solid State Communications, 39*(1), 159–161. https://doi.org/10.1016/0038-1098(81)91069-3

Liechtenstein, A. I., Mazin, I. I., Rodriguez, C. O., Jepsen, O., & Andersen, O. K. (1991). Structural phase diagram and electron-phonon interaction in $Ba_{1-x}K_xBiO_3$. *Physical Review B, 44*(10), 5388–5395. https://doi.org/10.1103/PhysRevB.44.5388

Mehl, M. J., Papaconstantopoulos, D. A., & Singh, D. J. (2001). Effects of C, Cu and Be substitutions in superconducting MgB_2. *Physical Review B, 64*(14), 140509. https://doi.org/10.1103/PhysRevB.64.140509

Papaconstantopoulos, D. A., Boyer, L. L., Klein, B. M., Williams, A. R., Morruzzi, V. L., & Janak, J. F. (1977). Calculations of the superconducting properties of 32 metals with $Z \leq 49$. *Physical Review B, 15*(9), 4221–4226. https://doi.org/10.1103/PhysRevB.15.4221

Rainer, D., & Sauls, J. A. (1992). Strong coupling theory of superconductivity. In S. K. Joshi, C. N. R. Rao, & S. V. Subramanyam (Eds.), *Superconductivity: From basic physics to the latest developments* (pp. 45–78). World Scientific. https://doi.org/10.1142/9789814503891_0002

Ranong, N. N., Natkunlaphat, N., & Pinsook, U. (2023). Simplified models for electron-phonon interactions in materials: Insights from theory and experimental data. *Journal of Physics: Conference Series, 2653*(1), 012060. https://doi.org/10.1088/1742-6596/2653/1/012060

Sahni, V., Bohnen, K.-P., & Harbola, M. K. (1988). Analysis of the local-density approximation of density-functional theory. *Physical Review A, 37*(6), 1895–1906. https://doi.org/10.1103/PhysRevA.37.1895

Salunke, H. G., Mittal, R., Das, G. P., & Chaplot, S. L. (1997). Electron–phonon coupling and related properties of C16-structured Zr_2Ni intermetallics. *Journal of Physics: Condensed Matter, 9*(46), 10137–10143. https://doi.org/10.1088/0953-8984/9/46/012

Savrasov, S. Y., & Andersen, O. K. (1996). Linear-response calculation of the electron-phonon coupling in doped $CaCuO_2$. *Physical Review Letters, 77*(21), 4430–4433. https://doi.org/10.1103/PhysRevLett.77.4430

Savrasov, S. Y. (1992). Linear-response calculations of lattice dynamics using muffin-tin basis sets. *Physical Review Letters, 69*(19), 2819–2822. https://doi.org/10.1103/PhysRevLett.69.2819

Savrasov, S. Y., & Savrasov, D. Y. (1992). Full-potential linear-muffin-tin-orbital method for calculating total energies and forces. *Physical Review B, 46*(19), 12181–12195. https://doi.org/10.1103/PhysRevB.46.12181

Savrasov, S. Y., & Savrasov, D. Y. (1996). Electron-phonon interactions and related physical properties of metals from linear-response theory. *Physical Review B, 54*(23), 16487–16501. https://doi.org/10.1103/PhysRevB.54.16487

Shang, H. (2021). The Sternheimer approach to all-electron real-space density-functional perturbation theory with atomic basis set. *AIP Advances, 11*(1), 015224. https://doi.org/10.1063/5.0029361

Van Loon, E. G. C. P., Rösner, M., Schönhoff, G., Katsnelson, M. I., & Wehling, T. O. (2018). Competing Coulomb and electron–phonon interactions in NbS_2. *npj Quantum Materials, 3*(1), 32. https://doi.org/10.1038/s41535-018-0105-4

Venderbosch, R. (2022). *Analysis of a generalised local-density approximation in density-functional theory* [Bachelor's thesis, Eindhoven University of Technology].

Welakuh, D. M., Flick, J., Ruggenthaler, M., Appel, H., & Rubio, A. (2022). Frequency-dependent Sternheimer linear-response formalism for strongly coupled light–matter systems. *Journal of Chemical Theory and Computation, 18*(7), 4354–4365. https://doi.org/10.1021/acs.jctc.2c00076

Winter, H. (1981). Application of linear response theory to electron-phonon coupling. *Journal of Physics F: Metal Physics, 11*(11), 2283–2296. https://doi.org/10.1088/0305-4608/11/11/011

Wolf, E. L. (2012). *Principles of electron tunneling spectroscopy* (2nd ed.). Oxford University Press.

Xie, S. R., Quan, Y., Hire, A. C., Deng, B., DeStefano, J. M., Salinas, I., Shah, U. S., Fanfarillo, L., Lim, J., Kim, J., Stewart, G. R., Hamlin, J. J., Hirschfeld, P. J., & Hennig, R. G. (2022). Machine learning of superconducting critical temperature from Eliashberg theory. *npj Computational Materials, 8*(1), 14. https://doi.org/10.1038/s41524-021-00666-7